JOURNAL OF SOLID STATE CHEMISTRY 102, 146–155 (1993)

Synthesis and Structure of $RbVP_2S_7$: A New Thiophosphate in the M^I–V–P–S Family

E. DURAND, M. EVAIN,* AND R. BREC

Laboratoire de Chimie des solides, Institut des Matériaux de Nantes, 2 rue de la Houssinière, 44072 Nantes Cédex 03, France

Received March 9, 1992; in revised form June 8, 1992; accepted June 24, 1992

$RbVP_2S_7$ has been obtained as black platelets by heating the elements in stoichiometric proportions at 550°C under vacuum in evacuated silica tubes for 21 days. It crystallizes in the monoclinic symmetry, space group $C2$, with the parameters $a = 858.30(9)$ pm, $b = 956.8(1)$ pm, $c = 646.94(3)$ pm, and $\beta = 98.22(1)°$, $V = 525.8(1) \times 10^6$ pm^3. The refinements led to a reliability factor of 2.7% for 933 independent reflections and 56 variables. The structure of $RbVP_2S_7$ is built from VS_6 octahedra and PS_4 tetrahedra. The tetrahedra, which form P_2S_7 groups through apex sharing, bind the VS_6 octahedra through mutual apexes or edges. The rubidium atom occupies the center of a sulfur bicapped trigonal prism, thus exhibiting a coordination of eight. Within its site, the rubidium important displacement can only be described by using a third-order anharmonic tensor (Prometheus program). The atomic distances and magnetic properties are in agreement with the $Rb^{I}V^{III}(P_2S_7)^{-IV}$ charge balance.

I. Introduction

In 1965, Hahn and Klingen (*1*) prepared and characterized a new family of compounds, the thiophosphates of transition elements MPS_3. In these phases a phosphorus IV implies the occurrence of a metal II; thus "VPS_3" was thought to present such an ion, although vanadium III is rather more stable in a sulfur environment. A more recent analytical and structural determination showed that, in fact, the exact formulation of the material was $V_{0.78}PS_3$ (*2*). The occurrence of vanadium deficiency corresponds to a mixed valence phase to be written $V^{III}_{0.44}V^{II}_{0.34}\square_{0.22}PS_3$. This characteristic is to be ascribed to a stability decrease of the II oxydation state when going from Zn to V. In effect, the energy levels of the transition metal *d* orbitals go up continuously, and a better stability (i.e., an electronic depletion of these orbitals) is then restored through a higher oxidation state. A still more stable situation is reached in the case of the vanadium derivative because of the electronic stabilization taking place by the setting up of an electronic hopping between V^{II} and V^{III}. Beyond vanadium, titanium is present as a Ti^{IV} species in TiP_2S_6 (*3*), the phase being then tridimensional. In the MPS_3 family, vanadium is clearly a border case with a similar stability for V^{II} and V^{III}. By substituting half of the vanadium by an M^I cation, it was thought possible to stabilize the higher vanadium oxidation state, and $AgVP_2S_6$ (*4*), $AgVP_2Se_6$ (*5*), and then $CuVP_2S_6$ (*6*) could be obtained. $AgVP_2S_6$, in which the cations are arranged in chains within the

* To whom correspondence should be addressed.

0022-4596/93 $5.00

TABLE I
SEM ANALYSIS RESULTS

Elements	Rb	V	P	S
Experimental (%)	7.35	8.48	19.61	64.56
Calculated (%) $RbVP_2S_6$	10.00	10.00	20.00	60.00
Calculated (%) $RbVP_2S_7$	9.09	9.09	18.18	63.64

two-dimensional slabs of the structure, is an excellent model compound to illustrate the Haldane conjecture (*7*). In the $MM'P_2X_6$ phases, the occurrence of silver and vanadium chains rather than the setting up of triangular distributions on a honeycomb sublattice is to be related to the bond length ratio $d_{M-X}/d_{M'-X}$ (*8–10*). For values higher than 1.13, the arrangement is chain-like, whereas for lower ones, it is triangular. With some IS group large cations (K, Rb, and Cs for instance), vanadium chains could be expected to form $M^IVP_2S_6$ phases, implying new magnetic behavior to be compared with existing chain-containing related phases. In an attempt to prepare such compounds, $RbVP_2S_7$ was obtained instead. This article describes the synthesis and structure determination of this new thiophosphate.

II. Experimental Section

1. Synthesis and Analysis

$RbVP_2S_7$ was prepared by direct synthesis from the elements heated in evacuated silica tubes at 550°C for 21 days. After a three day slow cooling, black platelets were obtained at the surface of a powdered bulk. If the single crystals corresponded well enough to the nominal composition $RbVP_2S_7$ rather than to the $RbVP_2S_6$ one (see Table I), the sample bulk was not pure at all. Attempts to obtain a large amount of the pure compound by changing the temperature and composition did not succeed.

The crystals of the phase were handled in air, since they did not show any reaction with oxygen and water, contrary to many alkali-metal-containing phases.

2. X-ray Powder Data and Single Crystal Studies

An X-ray diagram was obtained from ground single crystals sorted out from the sample bulk surface and using an INEL diffractometer equipped with a curve detector CPS120. Because of the presence of impurities, this diagram could not be indexed entirely. With the help of the single crystal structure determination (*vide infra*), and with the use of the theoretical powder diagram calculated with the Lazy Pulverix program (*11*), we could safely assign the diffraction lines belonging to $RbVP_2S_7$ (see Table II). A least-squares refinement led to the parameters a = 858.30(9) pm, b = 956.8(1) pm, c = 646.94(3) pm, β = 98.22(1)° and V = 525.8(1) × 10^6 pm^3 with a $\Delta 2\Theta_{mean}$ = 0.005°.

The sorting out of a proper single crystal for X-ray recording proved very difficult because of systematic twinning. On Weissenberg films, the splitting of the a^* axis was always found. This seems to correspond to the occurrence of microdomains, since it has been impossible to eliminate the twinning through cleavage of the crystals. It was then decided to record the diffracted intensities in the range $-h/h$, $0/k$, and $-l/l$ for the two system sets. The results of the structure determination given hereafter correspond to the more intense one. All the recordings were conducted on a Nonius four-circle CAD4-κ diffractometer. The cell parameters of the monoclinic cell, refined from 25 reflections, were a = 856.6(2) pm, b = 954.7(3) pm, c = 646.03(7) pm, and β = 98.23(1)°, in very good agreement with those yielded by the powder diagram (*vide supra*).

TABLE II

X-RAY POWDER DIFFRACTION OF $RbVP_2S_7$

d (obs) (pm)	d (calc) (pm)	h	k	l	I_{calc}[a]	I_{obs}[a]
640.30	640.30	0	0	1	58.9	100
477.26	477.18	1	1	−1	75.2	22
428.62	428.63	1	1	1	50.4	18
383.28	383.23	0	2	1	94.0	20
332.58	332.72	2	0	1	20.3	3
320.05	320.15	0	0	2	1.1	6
317.68	317.62	2	2	0	100.0	10
299.06	299.03	1	1	−2	20.5	18
275.95	275.96	1	3	−1	51.5	12
275.25	275.27	2	0	−2	73.8	33
274.34	274.35	1	1	2	32.5	33
273.13	273.15	2	2	1	73.6	15
271.54	271.52	3	1	0	33.4	4
266.04	266.06	0	2	2	15.5	12
263.32	263.28	3	1	−1	22.5	2
239.68	239.72	2	0	2	3.5	2
238.55	238.59	2	2	−2	9.7	4
224.03	224.04	1	3	−2	6.9	3
214.33	214.32	2	2	2	21.2	7
213.49	213.43	0	0	3	0.6	9
209.22	209.18	1	1	−3	4.6	9
194.94	194.92	3	3	1	2.4	10
	194.91	0	2	3	12.1	
194.20	194.21	2	4	1	45.2	7
186.64	186.63	2	2	−3	20.8	13
179.38	179.36	4	2	1	8.3	2
151.80	151.80	0	2	4	6.2	7
146.96	146.99	3	1	−4	3.9	5
144.10	144.12	1	3	−4	2.3	1
143.17	143.19	2	0	4	4.4	5
128.24	128.22	1	1	−5	1.9	3
123.05	123.05	4	6	1	3.7	2

[a] Intensities calculated with the Lazy Pulverix Program for a Debye–Scherrer geometry and without anomalous dispersion. Differences between I_{calc} and I_{obs} are mostly to be attributed to preferred orientation.

Table III gathers all the analytical and crystallographic data of the study.

3. *Structure Refinement*

All calculations and refinements have been made using the MOLEN (*12*) and Prometheus (*13*) chain programs. Since the twinning concerned only the (0*kl*) reciprocal planes, these were eliminated from the calculations. After usual corrections (Lorentz-polarization and psi-scan semiempirical absorption) of the 2414 recorded reflections, 933 independent reflections with $I > 2.5\,\sigma(I)$ were obtained. The refinement calculations were carried out in the $C2$ noncentrosymmetric space group. A $1/\sigma^2$ weighting scheme was chosen, with an instability factor of 0.04. The Patterson map easily revealed the rubidium positions, and succes-

TABLE III

ANALYTICAL AND CRYSTALLOGRAPHIC DATA. PARAMETERS OF THE X-RAY DATA COLLECTION AND REFINEMENT

Physical, crystallographic, and analytical data

Formula: $RbVP_2S_7$ — Molecular weight: 422.82 g/mol
Color: black
Crystal system: monoclinic — Space group: $C2$ (5)
Room temperature constants:
a = 858.3(9) pm, b = 956.8(1) pm, c = 646.94(3) pm
β = 98.22(1)° Z = 2
Density (calc.): 2.687
Absorption factor: $\mu(MoK\alpha)$ = 70.1 cm^{-1}

Data collection

Temperature: 298 K
Radiation: $MoK\alpha$ — Monochromator: oriented graphite (002)
Scan mode: $\omega/2\theta$ — Scan angle: 1.2 + 0.35tan(θ)
Recording range: 1.5–35°
Values determining the scan speed:
SIGPRE: 0.7 SIGMA: 0.01 VPRE: 3 min^{-1}
Standard reflections: 0 2 0, 0 0 4, −2 0 2 (every 3600 s)

Refinement conditions[a]

Reflections for crystal matrix orientation:		25
Recorded reflections in a ½ space:		2414
Independent reflections with $I > 2.5\sigma(I)$:		933
Refined parameters:	$N(1)$ =	52
	$N(2)$ =	56
Reliability factors:	$R = \Sigma(\lvert F_o\rvert - \lvert F_c\rvert)/\Sigma\lvert F_c\rvert$	
	$R_w = [\Sigma(w(\lvert F_o\rvert - \lvert F_c\rvert)^2)/\Sigma(w\lvert F_o\rvert^2)]^{1/2}$	
	$w = 1/\sigma^2$	

Refinement results[a]

$R(1)$ = 0.03108 $R_w(1)$ = 0.02448
$R(2)$ = 0.02752 $R_w(2)$ = 0.02123

EC(1): 1.2(2) × 10^{-6}
EC(2): 1.1(1) × 10^{-6}

ΔF + (1): 1.07 × 10^{-6} e^-/pm^3 ΔF − (1): −1.06 × 10^{-6} e^-/pm^3
ΔF + (2): 0.35 × 10^{-6} e^-/pm^3 ΔF − (2): −0.38 × 10^{-6} e^-/pm^3

[a] $N(1)$, $R(1)$, $R_w(1)$, ΔF − (1), ΔF + (1), and EC(1) are the number of refined parameters, the agreement factors, the minima and maxima in the difference Fourier map, and the extinction coefficient, respectively, after refinements with only harmonics ADPs; $N(2)$, $R(2)$, $R_w(2)$, ΔF − (2), ΔF + (2), and EC(2) are the equivalent results after including tensor elements up to the third order.

TABLE IV

POSITIONAL PARAMETERS AND THEIR ESTIMATED STANDARD DEVIATION FOR THE SPLIT MODEL WITH TWO RUBIDIUM ATOMS AND HARMONIC ATOM DISPLACEMENT PARAMETERS

Atom name	X	Y	Z	B_{eq}[a] $\times 10^4$ pm^2
Rb1 0.90	0	0.8880(5)	$\frac{1}{2}$	3.00(2)
Rb2 0.10	0	0.942(3)	$\frac{1}{2}$	2.6(2)
V	$\frac{1}{2}$	0	0	1.26(2)
P	0.3023(1)	0.6465(1)	0.9173(2)	1.15(1)
S1	0.65889(9)	0.0266(1)	0.7154(1)	1.54(2)
S2	0.3074(1)	0.1658(1)	0.8275(2)	1.72(2)
S3	0.3658(1)	0.8180(1)	0.7709(2)	1.87(2)
S4	0	0.0122(2)	0	1.55(2)

Note. The filling ratio is given for each rubidium atom.

[a] Isotropic equivalent ADP defined as B_{eq} (pm^2) = $\frac{4}{3}\Sigma_i\Sigma_j\beta_{ij}a_ia_j$.

sive Fourier and difference Fourier maps led to the other atoms locations. A first series of cycles were performed using isotropic atomic displacement parameters (ADP). The ADP labeling is now used instead of the classical atomic thermal parameter (ATP) one, because it is more general, including in particular atomic disorder. Before introducing the anisotropic ADPs, the calculations were carried out by transforming the x, y, z atomic coordinates into $-x, -y, -z$. The refinement leading to the lower reliability R factor was subsequently considered as representing the actual atomic configuration. After introducing the anisotropic ADPs, the R value dropped from 5.1 to 3.1% for 52 variables. However, a last Fourier map revealed nonnegligible residues of the electronic density around the rubidium position. In addition, the ADP value along one direction (U_{22} = 0.073 $\times$ 10^4 pm^2) was about twice as high as the ADP along the other two (U_{11} = 0.032 $\times$ 10^4 pm^2 and U_{33} = 0.027 $\times$ 10^4 pm^2). At that step of the calculation procedure, we decided to use a split model to describe the alkali-metal site, and a second position, away by about 50 pm along the y axis, was introduced. The refinement was carried on, the occupancy ratio (τ) of the two rubidium positions being set free. This model led to a majority site (Rb1 with τ = 0.90) and a minority one (Rb2 with τ = 0.10). Anisotropic ADPs were used for Rb1, whereas Rb2 was kept isotropic. After a few cycles, the confidence factors set to R = 2.78% (R_w = 2.14%) for the 933 reflections, and using 55 variables (see in Table IV the atomic parameters and B_{eq} values). A joint probability density function (*jpdf*) was then calculated around the Rb sites in the plane (*ab*) (Fig. 1) and an effective one particle potential (OPP) along the *b* axis (Fig. 2). They showed that the refined majority position Rb1 (defined as "mean" (*14*)) almost coincides with the maximum probability (referred to as "mode" (*14*)), whereas the second position Rb2 introduces a distortion in the majority curve along the *b* axis.

Instead of keeping this split model, for which dual positions are physically meaningless but correspond to a disorder, it is possible to introduce a single site with an

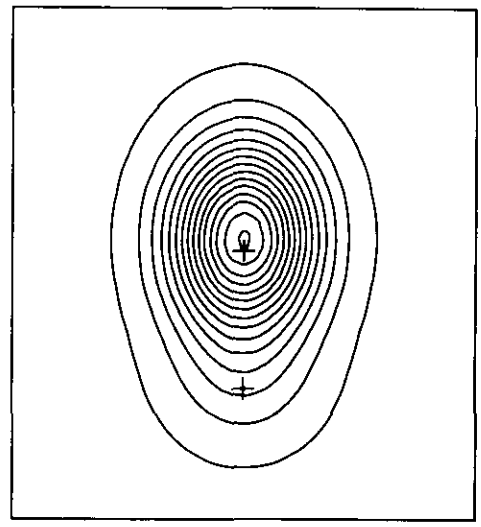

FIG. 1. Joint probability density function (*jpdf*) calculated around the rubidium atom positions in the (*ab*) plane for $RbVP_2S_7$. This *jpdf* corresponds to the calculation with a split model (two rubidium sites).

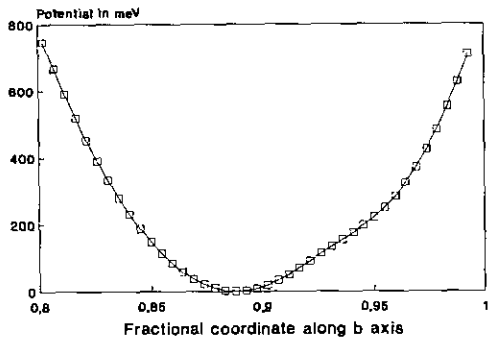

FIG. 2. Effective one particle potential (OPP) around the rubidium site and along the b axis in $RbVP_2S_7$ with the split model calculation.

TABLE V

POSITIONAL PARAMETERS AND THEIR ESTIMATED STANDARD DEVIATION FOR THE MODEL WITH ONE RUBIDIUM ATOM AND ANHARMONIC REFINEMENT

Atom name	X	Y	Z	B_{eq}[a] $\times 10^4$ pm^2
Rb	0	0.8938(2)	$\frac{1}{2}$	3.51(2)
V	$\frac{1}{2}$	0	0	1.25(1)
P	0.3023(1)	0.6466(1)	0.9174(2)	1.13(2)
S1	0.65887(9)	0.0266(1)	0.7155(1)	1.54(2)
S2	0.3074(1)	0.1658(1)	0.8275(2)	1.70(2)
S3	0.3658(1)	0.8180(1)	0.7709(2)	1.87(2)
S4	0	0.0123(2)	0	1.54(2)

[a] Isotropic equivalent ADP defined as B_{eq} (pm^2) = $\frac{4}{3}$ $\Sigma_i\Sigma_j\beta_{ij}a_ia_j$.

anharmonic ADP. We then used such an ADP with a third-order tensor based on the Gram–Charlier formalism (*15*),

$$T(\mathbf{H}) = T_{harm}(\mathbf{H})\,[1 + (2\pi i)^3/3!\,C^{pqr}h_p h_q h_r]\ (16),$$

(using Einstein's sum convention) where h_p, h_q, and h_r are the Miller indices, C^{pqr} is an element of the third-order tensor, and $i^2 = -1$. An imaginary component in the displacement factor introduces the occurrence of a non-centrosymmetric probability density function. With this model, the R factor went down to 2.75% (R_w = 2.12%) for 56 variables. At the same time, the residual maxima of the fourier difference map dropped significantly (see Table III). In addition the correlations diminished. The result, compared to that obtained with the previous model, justifies the use of a single atomic rubidium position to model the structure of $RbVP_2S_7$. The atomic parameters and the equivalent isotropic ADP are gathered in Table V. The anisotropic ADPs (U_{ij}) are reported in Table VI. Those of rubidium, with the components of the anharmonic third-order tensor, are in Table VII. To compare these results with the split model ones, a *jpdf* and an OPP were calculated (Figs. 3 and 4). The noncoincidence of the "mode" and the "mean" reveals its asymmetry.

III. Structure Description and Discussion

$RbVP_2S_7$ structure can be described as deriving from two-dimensional slabs between which are located the rubidium ions that bond them together. The slabs are made of VS_6 octahedra and PS_4 tetrahedra, represented in Fig. 5. The rubidium trigonal prismatic bicapped surrounding is built from three VS_6 octahedra from each of the neighbor slabs. Between two VS_6 octahedra are found either a PS_4 group or a P_2S_7 unit made from two apex-sharing PS_4 tetrahedra. The VS_6 octahedra thus share one edge or one apex with the PS_4 tetrahedra (Figs. 6 and 7).

TABLE VI

ADP: SECOND-ORDER TENSOR ELEMENTS $U(i,j)$ (pm^2)

Atom name	$U(1,1)$	$U(2,2)$	$U(3,3)$	$U(1,2)$	$U(1,3)$	$U(2,3)$
Rb	321(3)	750(6)	273(4)	0	51(3)	0
V	134(3)	152(4)	194(5)	0	39(3)	0
P	117(3)	151(4)	165(4)	−14(3)	18(3)	12(4)
S1	158(3)	240(5)	187(4)	−56(4)	33(3)	−45(4)
S2	225(4)	218(5)	231(5)	62(4)	104(4)	76(4)
S3	258(4)	201(4)	231(6)	−86(4)	−27(4)	49(4)
S4	140(5)	164(6)	272(7)	0	−2(4)	0

Note. The form of the anisotropic displacement parameter is: $\exp[-2\pi^2(h^2a^{*2}U(1,1) + k^2b^{*2}U(2,2) + l^2c^{*2}U(3,3) + 2hka^*b^*U(1,2) + 2hla^*c^*U(1,3) + 2klb^*c^*U(2,3))]$.

TABLE VII

ADP: SECOND ($U(i, j)$) AND THIRD ($C(p, q, r)$) ORDER ANHARMONIC TENSOR ELEMENTS FOR RUBIDIUM

	Rb
$U(1,1)^a$	321(3)
$U(2,2)$	750(6)
$U(3,3)$	273(4)
$U(1,2)$	0
$U(1,3)$	51(3)
$U(2,3)$	0
$C(1,1,1)^b$	0
$C(2,2,2)$	0.0109(6)
$C(3,3,3)$	0
$C(1,1,2)$	0.0005(3)
$C(1,2,2)$	0
$C(1,1,3)$	0
$C(1,3,3)$	0
$C(2,2,3)$	0
$C(2,3,3)$	−0.0000(5)
$C(1,2,3)$	0.0005(3)

[a] $U(i,j)$ in pm^2.

[b] Third-order tensor elements $C(p,q,r)$ have been multiplied by 10^3.

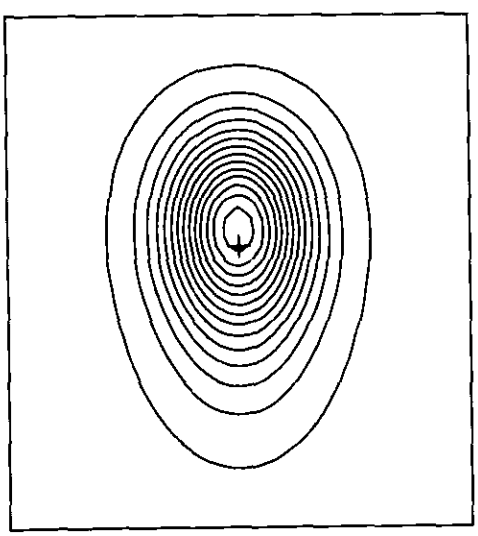

FIG. 3. *jpdf* calculated around Rb^I in the (*ab*) plane in $RbVP_2S_7$ for the anharmonic model, with one position and a third-order tensor.

If one considers the VS_6 octahedral angles (see Table VIII), it can be inferred that the units are strongly distorted, although the V–S length dispersion remains small (245.3(1), 245.8(1), and 243.8(1) pm). The mean V–S distance (245.0 pm) allows us to calculate a mean ionic radius for vanadium of 61 pm, considering an effective radius for sulfur of $r_{S^{-II}}$ = 184 pm. This agrees well with a V^{III} cation in octahedral sulfur environment for which the literature reports a value of $r_{V^{III}}$ = 64 pm (*17*). In addition, if one refers to the curve of the oxydation state variation versus the ionic radius for vanadium in some sulfides and selenides (*6*), this value falls very well on the straight line.

In its bicapped surrounding (see Figs. 6 and 7), the rubidium atom shows two sets of distances (they are calculated using the atomic position of the mean, which are not in any case very far from that of the mode). The shorter Rb–S ones are those between Rb^I and the sulfur ions forming the capping (2 × 343.7(1) pm) and the common sulfur of the P_2S_7 units (2 × 342.82(7) pm). The longer Rb–S bond lengths are those which involve the sulfur atoms bonding the VS_6 octahedra (2 × 364.7(1) and 2 × 358.2(1) pm). The average rubidium radius is equal to 168 pm, in rather satisfactory agreement with the reported value of 161 pm (*17*). If one considers that the shorter distances are more repre-

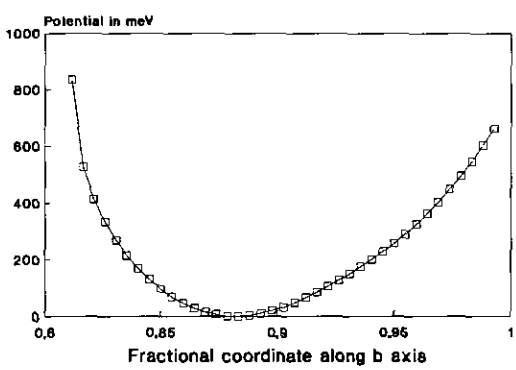

FIG. 4. Effective OPP along the *b* axis for the anharmonic refinement.

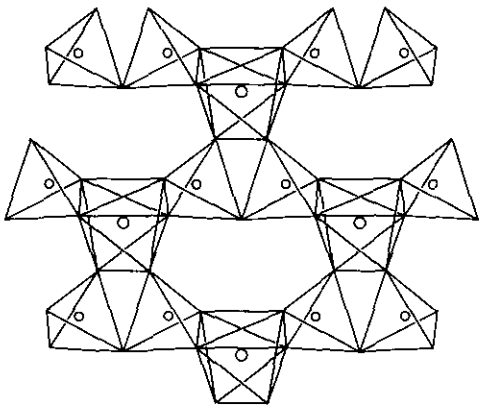

FIG. 5. $RbVP_2S_7$ structural arrangement within the compound constituting slab. The VS_6 octahedra are linked through P_2S_7 anionic bi-tetrahedral units (small and large open circles represent the phosphorus and vanadium atoms, respectively).

TABLE VIII

MAIN INTERATOMIC DISTANCES (pm) AND ANGLES (°) IN $RbVP_2S_7$

P–S:	P–S1		201.6(2)	P–S–P:	P–S4–P		105.77(9)
	P–S2		202.1(2)				
	P–S2		202.1(2)	S–P–S:	S1–P–S2		105.55(6)
	P–S3		200.3(2)		S1–P–S3		109.83(8)
	P–S3		200.3(2)		S1–P–S4		102.06(7)
	P–S4		213.3(1)		S2–P–S3		120.04(8)
					S2–P–S4		107.21(7)
					S3–P–S4		110.56(7)
V–S:	V–S1	(×2)	245.3(1)	S–V–S:	S1–V–S2	(×2)	90.09(4)
	V–S2	(×2)	243.8(1)		S1–V–S2	(×2)	82.18(4)
	V–S3	(×2)	245.8(1)		S1–V–S3	(×2)	83.30(4)
					S1–V–S3	(×2)	85.01(4)
	$V–S_{av}$		245.0		S2–V–S3	(×2)	87.49(4)
					S2–V–S2		99.06(7)
					S3–V–S3		90.06(2)
Rb–S:	Rb–S1	(×2)	364.7(1)				
	Rb–S2	(×2)	358.2(1)				
	Rb–S3	(×2)	343.7(1)				
	Rb–S4	(×2)	342.82(7)				
	$Rb–S_{av}$		352.3				

sentative of a regular Rb–S bonding, then a 159 pm radius is obtained, closer to the literature value. In any case, both distances are in the expected variation range.

The reason for the anharmonic behavior of rubidium in its site may be related to various factors. The first one is the small ligand field stabilization induced by the ligand field on that spherical ion. The second is the weak ionicity of the structure, implying a relative freedom of displacement of the cation without much crystal energy difference. Finally, the large asymmetrical cage (the biprism is only bicapped) probably allows for several favorable positioning with the coordination polyhedra.

Since phosphorus is located in PS_4 tetrahedra in P_2S_7 bitetrahedral units, it must be considered as a P^V species, leading to the overall charge balance for the phase $Rb^{I}V^{III}(P_2S_7)^{-IV}$. The P–S distances within the tetrahedra (201.6(2), 202.1(2), 200.3(2), and 213.3(1) pm) are in good accord with those calculated in $Ag_4P_2S_7$ (18) or $Hg_2P_2S_7$ (*19*), for instance, for the same anionic groups.

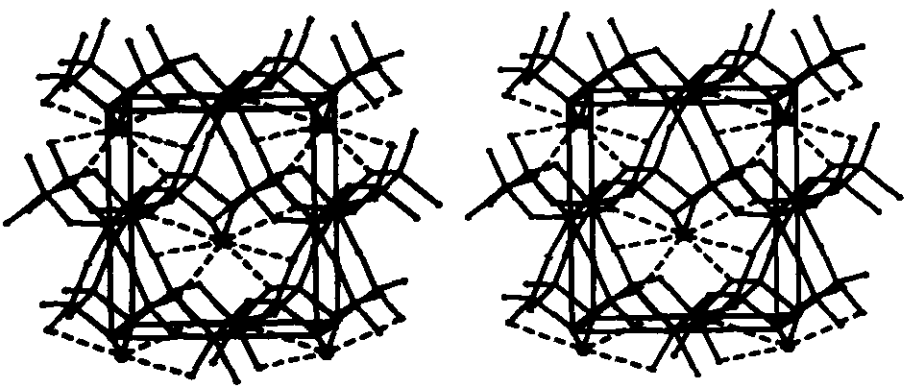

FIG. 6. $RbVP_2S_7$ stereoscopic view along the c axis. Rubidium atoms are represented by small open circles. The broken lines symbolize the Rb–S bondings. The trigonal prismatic bicapped coordination of Rb^{I} is clearly evidenced between the (VP_2S_7) slabs.

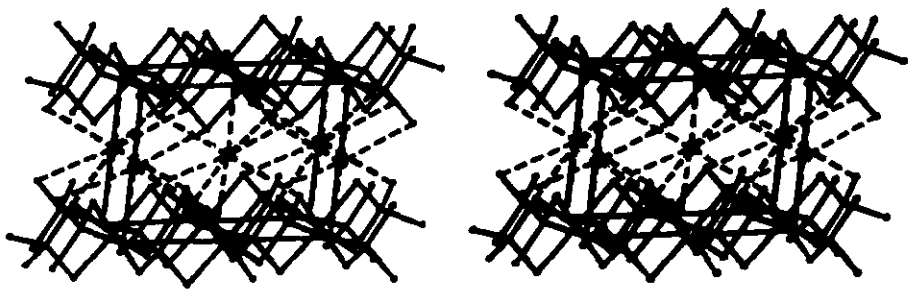

FIG. 7. $RbVP_2S_7$ stereoscopic view along the *b* axis showing the interslab localization of the rubidium ions. Rubidium atoms are represented by small open circles. The broken lines symbolize the Rb–S bondings.

Some of the S–P–S angles depart strongly from the ideal value of 109.45° (see Table VIII), implying that the PS_4 tetrahedra are far from regular. In addition, the P–S–P angle of 105.77(9)° which joins two phosphorus of two adjacent tetrahedra of the same $(P_2S_7)^{4-}$ unit, to be compared to 113.4° in $Ag_4P_2S_7$ and 108.6° in $Hg_2P_2S_7$, indicates clearly the amplitude of the relative tilt of two tetrahedra with respect of the straight alignment of 180°.

The thiodiphosphates and diphosphates have in common the presence of three shorter and one longer P–*X* bonds. This last one corresponds to the sulfur common to two tetrahedra. For instance, in $NaVP_2O_7$ (*20*), $RbVP_2O_7$ (*21*), $CsMoP_2O_7$ (*22*), $As_2P_2S_7$ (*23*), $Ag_4P_2S_7$ (*18*), and $Ag_7(PS_4, P_2S_7)$ (*24*), the bond length difference varies between 4 and 6%. With a variation of 5.5%, $RbVP_2S_7$ sits in the observed average.

IV. Magnetic Properties

To check the oxidation state of the vanadium cation in $RbVP_2S_7$, magnetic susceptibility measurements were carried out on a Faraday balance in the 80–450 K temperature range. The powder sample was obtained from ground selected single crystals. Figure 8 shows the reciprocal magnetic susceptibility (corrected from core diamagnetism) versus temperature. It appears that the compound does not obey a Curie–Weiss law and that it is not possible to calculate the number of unpaired electrons born by V^{III}, although it is clear that the phase contains localized moments. This is often observed in the case of d^2 cations. In effect, one is dealing with an intermediary situation between a spin only V^{III} and a true $^3T_{1g}$ (ideal O_h symmetry). This is in accord with the above structural distortions of the VS_6 octahedron. The V–S distance dispersion being weak, there is probably here no complete

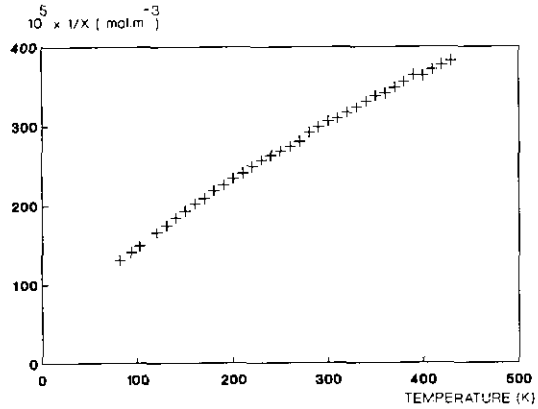

FIG. 8. Reciprocal molar susceptibility of $RbVP_2S_7$ versus temperature in the 80–450 K range.

decomposition of the $^3T_{1g}$ term in three separated levels.

V. Conclusion

The attempt to prepare a new substituted MPS_3 compound $Rb^IV^{III}P_2S_6$ failed, and it was $Rb^IV^{III}P_2S_7$ which was obtained instead. This may be found to be strange since Rb^I can be encountered in a variety of coordinations from VI to XIV, that expected in a classical $MM'P_2S_6$ phase being VI. However, the Rb^I ionic radius in an octahedral sulfur coordination is rather large (152 pm) (*17*) (it is to be recalled that $r_{Ag}I$ = 101 pm). This is probably too large to lead to the expected structural model with cationic chains like those encountered in $AgVP_2S_6$. This is certainly why the structure and composition are changed to coordinate Rb^I with a bicapped prism. In addition, the new phase presents a phosphorus cation at the oxydation state of V, and not IV (occurrence of P_2 pairs) as in the MPS_3 family.

It is important to point out that one observes a very high equivalent ADP value for Rb^I (3.51×10^4 pm^2) in accord with the filled electronic outer configuration $3d^{10}3p^6$ of the alkali-cation. This behavior, systematically observed for M^I ID elements (Cu, Ag), seems to occur also with alkali-metals. This often implies a split model description or an anharmonic treatment or a hybrid model (*25*). In the present case, a description allowing a noncentrosymmetric ADP (tensor order of three) yielded the best results, while keeping only one rubidium site, i.e., a physically meaningful description of the structure.

Some compounds of the $M_xP_2S_7$ family (M = Ag, Hg, As, x = 2, 4) are quite well known, but this is the first time that a substituted derivative of this series has been synthesized. The host structure presents the advantage of accepting large trigonally coordinated cations, and it is certainly possible to widen this family with larger cation like Cs, Tl, Ba, . . . , by using a host cation M^{III} or M^{II} known to be particularly stable in an octahedral sulfur environment.

References

1. H. Hahn and W. Klingen, *Naturwissenschaften* **52,** 494 (1965).
2. G. Ouvrard, R. Freour, R. Brec, and J. Rouxel, *J. Mater. Res. Bull.* **20,** 1053 (1985).
3. W. M. J. Jandali, G. Eulenberger, and H. Hahn, *Z. Anorg. Allg. Chem.* **470,** 39 (1980).
4. S. Lee, P. Colombet, G. Ouvrard, and R. Brec, *J. Mater. Res. Bull.* **21,** 917 (1986).
5. G. Ouvrard and R. Brec, *J. Mater. Res. Bull.* **23,** 1199 (1988).
6. E. Durand, G. Ouvrard, M. Evain, and R. Brec, *Inorg. Chem.* **29,** 4916 (1990).
7. H. Mutka, J. Soubeyroux, G. Bourleaux, and P. Colombet, *Phys. Rev. B* **39,** 4820 (1989).
8. A. Leblanc, J. Rouxel, *C. R. Acad. Sci. Paris Ser. C* **291,** 12, 263 (1980).
9. P. Colombet, A. Leblanc, M. Danot, and J. Rouxel, *J. Solid State Chem.* **41,** 174 (1982).
10. P. Colombet, A. Leblanc, M. Danot, and J. Rouxel, *Nouv. J. Chim.* **7,** 333 (1983).
11. R. Yvon, W. Jeitschko, and E. Parthé, *J. Appl. Crystallogr.* **10,** 73 (1977).
12. C. Kay Fair, MOLEN: Structure Determination Package, Enraf–Nonius (1982).
13. U. H. Zucker, E. Perenthaler, W. F. Kuhs, R. Bachmann, and H. Schulz, *J. Appl. Crystallogr.* **16,** 358 (1983).
14. W. F. Kuhs, *Acta Crystallogr. Sect. A* **39,** 148 (1983).
15. C. K. Johnson and H. A. Levy, "International Tables for X-Ray Crystallography," Vol. IV, p. 316, Kynoch Press, Birmingham, (1974).
16. T. Hibma, *Solid. State. Commun.* **33,** 445 (1980).
17. R. D. Shannon, *in* "Structure and Bonding in Crystals" (M. O'Keeffe and A. Navrotsky, Eds.), Vol. 2, p. 61, Academic Press, New York (1981).
18. P. Toffoli, P. Khodadad, and N. Rodier, *Acta. Crystallogr. Sect. B* **33,** 1492 (1977).
19. M. Z. Von, G. Jandali, H. Eulenberg, and H. Hahn, *Z. Anorg. Allg. Chem.* **445,** 184 (1978).
20. Y. P. Wang, K. H. Lii, and S. L. Wang, *Acta Crystallogr. Sect. C* **45,** 1417 (1989).
21. U. Flörke, *Z. Kristallogr.* **191,** 137 (1990).
22. K. H. Lii and R. C. Hausalter, *Acta Crystallogr. Sect. C* **43,** 2036 (1987).
23. W. Hönle, C. Wibbelmann, and W. Brockner, *Z. Naturforsch. B.* **39,** 1088 (1984).
24. P. Toffoli, P. Khodadad and N. Rodier, *Acta. Crystallogr. Sect. B* **38,** 2374 (1982).
25. A. van der Lee, F. Boucher, M. Evain, R. Brec, and J. Rouxel, *Z. Kristallogr.* to appear.